

# SIMULATION MODEL FOR ADSORPTION BASED HYDROGEN STORAGE

Viktorija HABERL<sup>1\*</sup>, Elias M. HENÖGL<sup>1</sup>, Nejc KLOPČIČ<sup>1</sup>, Franz WINKLER<sup>1</sup>,  
Alexander TRATTNER<sup>1,2</sup>

1) HyCentA Research GmbH, Inffeldgasse 15, A-8010, Graz, +43 316 873 9500,  
office@hycenta.at, [www.hycenta.at](http://www.hycenta.at)

2) Graz University of Technology, Institute of Thermodynamics and Sustainable  
Propulsion Systems, Inffeldgasse 19, A-8010, Graz, trattner@tugraz.at,  
[www.ivt.tugraz.at](http://www.ivt.tugraz.at)

## **Abstract:**

In this work a 0D simulation model of the adsorption behaviour of hydrogen on activated carbon AX-21<sup>TM</sup> has been created, employing the modified Dubinin-Astakhov model [1], to perform parameter studies on the influences of the adsorption isotherms, the operation temperature, the temperature control and the mass flow, on the inside pressure, the total hydrogen storage capacity, the hydrogen mass distribution (adsorbed and in gas phase) and the filling time. The structure of the simulation framework will be explained in detail and the interdependency of the system parameters will be worked out for different scenarios. It is shown that the operation of an adsorption storage tank at cryogenic temperatures (77 K) significantly enhances the total storage capacity, compared to operation at room temperature. Optimizing the temperature control with regards to the thermal conductivity results in a more effective heat dissipation and leads to operation temperatures closer to the target temperature. Different mass flows have only very little influence on the filling time when loading the tank fully, due to a self-limiting thermal behaviour, while for partial tank filling, higher mass flows result in much faster filling times. It is also shown that the adsorption time constant used in the linear driving force model [2] greatly influences the mass distribution (the ratio of stored adsorbate to stored gas phase) and represents the crucial factor concerning the accurate representation of the adsorption kinetics of a real system.

**Keywords:** hydrogen, adsorption storage, activated carbon, 0D simulation model, adsorption isotherm

## **1 Introduction**

The worldwide need for energy is growing constantly. Our society is currently built on the use of fossil fuels to meet this energy demand. The excessive use of fossil fuels accelerates climate change by producing vast amounts of greenhouse gases. To decarbonise the energy system, fossil fuels need to be replaced with alternate carbon neutral energy carriers. For this undertaking, hydrogen has proven to be a promising candidate [3]: it has a higher gravimetric energy density than gasoline (gravimetric energy density of gasoline: 12.2 kWh/kg [4], gravimetric energy density of hydrogen: 33.3 kWh/kg [3]) and can be produced through water electrolysis from renewable energy. The end product of utilizing hydrogen as an energy carrier for fuel cells is water without any byproducts that harm the environment [5].

One of the key aspects for transitioning to a sustainable hydrogen society is the storage of hydrogen with high energy density. Hydrogen can be stored in liquid or gaseous form or sorbed into/onto solids, with each form posing its own challenges: Whilst liquid hydrogen has a higher volumetric energy density (2.2 kWh/l) than compressed hydrogen (1.3 kWh/l at 700 bar) [3], the energy needed for cooling to cryogenic conditions (about 20 K) is substantial [3] [6] and boil-off losses can be significant (0.3 - 3 % of hydrogen mass per day) [3].

Compressed hydrogen storage is feasible at room temperature, however the pressure needed, gives rise to safety concerns [3]. Sorption methods have the advantage of operating at higher temperatures than liquid hydrogen storage and at pressures below compressed hydrogen storage [3], whilst achieving gravimetric storage densities of up to 8.1 wt% (in activated carbon at 20 bar and 77 K) [7].

Two main categories of sorption-based hydrogen storage are to be differentiated: **absorption**- and **adsorption**-based storage. Absorption, on the one hand, is a bulk phenomenon, hydrogen is chemically bound and stored within the lattice of the metal alloy, forming a metal hydride. [3] Adsorption, on the other hand, is a surface phenomenon, based on weaker van der Waals forces and hydrogen is aggregated on the surface and inside the pores of the adsorbent [8].

Ideally, a storage vessel provides a high volumetric and gravimetric energy density and thus a large total storage capacity. Hydrogen uptake and release should be feasible close to ambient conditions with respect to temperature and pressure. Binding energy should be low enough to minimize the heat energy needed for desorption, but also providing enough binding energy to contain the hydrogen around room temperature. (Modification of carbon materials for efficient hydrogen storage at room temperature is a current topic in material research [9]) Uptake and release rates should achieve filling performances comparable to those of fossil fuel tanks. The adsorption material should be readily available, sustainably sourced and energy-efficiently produced, with the material being non-toxic, having a long lifetime (low degradation) and being recyclable after the end of life. Additionally, low maintenance of the individual components as well as the entire system is desired. Lastly, scalability and integration into pre-existing system layouts play a particularly important role in establishing adsorption-based hydrogen storage in the mobility sector, since storage vessels should be adaptable to various vehicle types.

To tackle these challenges the characteristic operation parameters are to be identified and their interrelations determined. With the impact that each parameter has on the system identified, the properties of the storage system can be tuned to enhance specific aspects. In this work we will focus on the operation temperature, the temperature control, the storage capacity as well as the mass flow and its related filling times.

For an estimation of the interrelations of these system parameters a MATLAB Simulink 0D adsorption storage tank model, based on the simulation model for metal hydride hydrogen storage by Klopčič et al. [10], has been created. It allows for a fast evaluation of the impact that different operation conditions have on the storage capacity, the thermal management and the filling time.

## 2 Methodology

The following section covers the description of the working principle of the MATLAB Simulink 0D model of hydrogen adsorption storage in activated carbon AX-21™, explaining the underlying theoretical concepts in the process. In the first subsection, the adsorption storage material is characterized and the concept of adsorption isotherms and how to display them in

a functional relation is explained. In the second subsection, the 0D tank model is presented based on a block diagram.

## 2.1 Adsorption storage material

The adsorption storage material under investigation is the activated carbon AX-21™. Its characteristic set of properties, measured by Richard et al. [1], is listed in Table 1. These properties greatly influence the adsorption storage behaviour in respect to temperature and pressure as it is stated in Chahine's rule for microporous activated carbons. The rule describes a linear relation between the hydrogen uptake and the pore volume and the surface area of the storage material. [11] This means, that adsorption materials with a high specific surface area and a low bulk density reach high storage capacities, as it is the case for AX-21™ classified as a high porosity activated carbon. These activated carbons have specific surface areas of up to 3000 m<sup>2</sup>/g. (in contrast, regular grade activated carbons only have specific surface areas of 700 m<sup>2</sup>/g to 1800 m<sup>2</sup>/g) [12]. AX-21™ has a bulk density of 0.3 g/cm<sup>3</sup> [1] which is one order of magnitude smaller than the density of dense graphite (2.26 g/cm<sup>3</sup>) [13].

The characteristic adsorption behaviour is experimentally derived by a set of measurements and depicted in the form of adsorption isotherms correlating the stored adsorbate to the tank pressure for constant temperatures.

Table 1: Material properties of the adsorption material AX-21™ [1]

| AX-21™                |                        |
|-----------------------|------------------------|
| Specific surface area | 2800 m <sup>2</sup> /g |
| Bulk density          | 0.3 g/cm <sup>3</sup>  |
| Specific void volume  | 2.9 cm <sup>3</sup> /g |

To implement an adsorption material into the simulation model, the adsorption behaviour of the material must be described via a functional relation. This is achieved by fitting experimentally determined adsorption isotherms mentioned above, to a suitable isotherm model.

A model, that has proven a good data representation, is the modified Dubinin-Astakhov model (D-A model). It relates tank temperature ( $T$ ) and the tank pressure ( $P$ ) to the absolute adsorption ( $n_{ads}$ ) via the functional relation shown in Equation (1). The corresponding fit parameters are listed in Table 2.  $R$  is the universal gas constant. [1]

Table 2: Modified Dubinin-Astakhov fit parameters for adsorption isotherms of AX-21™ [1]

Modified D-A fit parameters

|           |              |
|-----------|--------------|
| $n_{max}$ | 71.6 mol/kg  |
| $P_0$     | 1470 MPa     |
| $\alpha$  | 3080 J/mol   |
| $\beta$   | 18.9 J/mol K |

$$n_{ads} = n_{max} * \exp\left[-\left[\frac{RT}{\alpha + \beta T}\right]^2 \ln^2\left(\frac{P_0}{P}\right)\right] \quad (1)$$

The resulting D-A function of the absolute hydrogen adsorption isotherms on AX-21™ is shown in Figure 1. The specific stored amount of adsorbate (hydrogen), normalized to 1 kg of adsorption storage material (AX-21™), is plotted over the tank pressure. For a constant temperature of e.g. 77 K more adsorbate is deposited into/onto the material with increasing tank pressure. While the initial adsorption rate (at low pressure) is high, the isotherms show a significant flattening at higher pressure (at constant temperature) showing a saturation behaviour where the isotherms asymptotically approach a maximum value of stored adsorbate ( $n_{max}$ ). Contrarily, the higher the tank temperature the fewer adsorbate can be stored at the same tank pressure. With adsorption energies for hydrogen on activated carbon being between 6 and 8 kJ/mol, high storage capacities can only be reached at low temperatures [8].

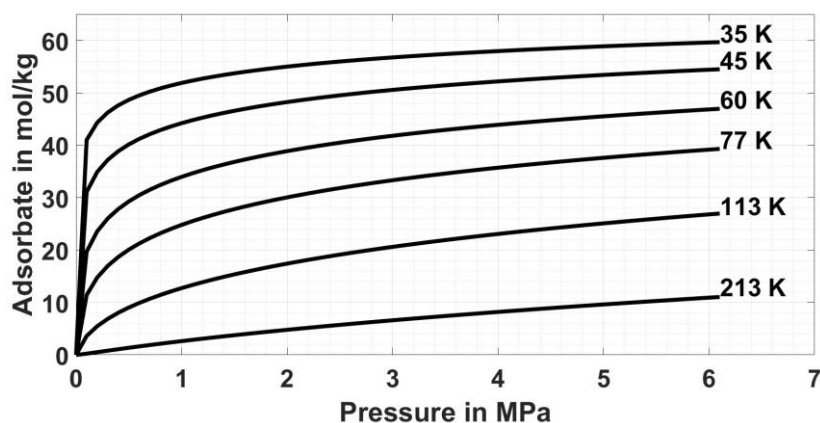


Figure 1: Simulated adsorption isotherms of AX-21™ for different temperatures, employing the modified Dubinin-Astakhov model (Equation (1)) with fit parameters from [1]

Since the concept of absolute adsorption only holds for adsorption processes at low pressure and high temperatures [1], the theory has to be adapted for adsorption tanks operated at higher pressures, such as in the following examples, by introducing the concept of excess adsorption, which will be discussed in the following.

For adsorption storage tanks operated at high pressures the experimentally determined adsorption isotherms will not coincide with the absolute adsorption isotherms. [1] Experiments

show an increase in stored adsorbate up to a certain pressure, where the stored mass appears to decrease when pressure is increased further, instead of the saturation behaviour discussed before. The measured amount of adsorbed hydrogen is referred to as excess adsorption. The concept of excess adsorption provides an explanation for this experimentally observed phenomenon.

The amount of stored adsorbate is determined as the difference between the total mass of hydrogen in the tank (determined by filling the tank with a known mass flow) and the hydrogen stored in the gas phase (determined by the gas equation for the accessible volume, temperature and pressure of the tank). [14] If the gas phase volume was equal to the void volume of the storage material one would experimentally observe the absolute adsorption isotherm. However, the void volume is split up into two parts. One part is a pore volume or surface covering filled with adsorbed hydrogen (adsorption volume) and the other part is the volume available for the gas phase. Due to this "reduced" actual gas phase volume the measured tank pressure leads to an overestimation of stored gas phase, when the adsorption volume is not considered. The indirect determination of the adsorbed amount from the stored gas phase yields a wrong value because the volume, taken up by the adsorbate, is not accounted for. [1]

After correcting the excess adsorption for this amount of hydrogen one arrives at the absolute adsorption as depicted in Figure 1. For a more detailed explanation of the concept of excess adsorption and its mathematical derivation consult Richard et al. [1]. In this work the excess adsorption is accounted for by setting the specific gas phase volume as the difference between the specific void volume ( $2.9 \text{ cm}^3/\text{g}$ ) and the specific adsorption volume. The specific adsorption volume (in relation to the adsorbent mass) is derived by fitting the experimentally observed excess adsorption data to the D-A model adapted for excess isotherms. The specific adsorption volume is found to be  $1.43 \text{ cm}^3/\text{g}$ . As a result, the specific gas phase volume ( $V_{gas}$ ) amounts to  $1.47 \text{ cm}^3/\text{g}$ . [1]

## 2.2 0D tank model

In this section the sequence of steps of the simulation model is explained on the basis of the block diagram shown in Figure 2. The block diagram is described from top to bottom, starting with the tank dimensioning and defining the input and system parameters, followed by the description of the condition for permitting mass flow into the tank and the check for equilibrium conditions, then discussing the search for the equilibration target and finishing with the segment on determining the actual mass transferred per time step.

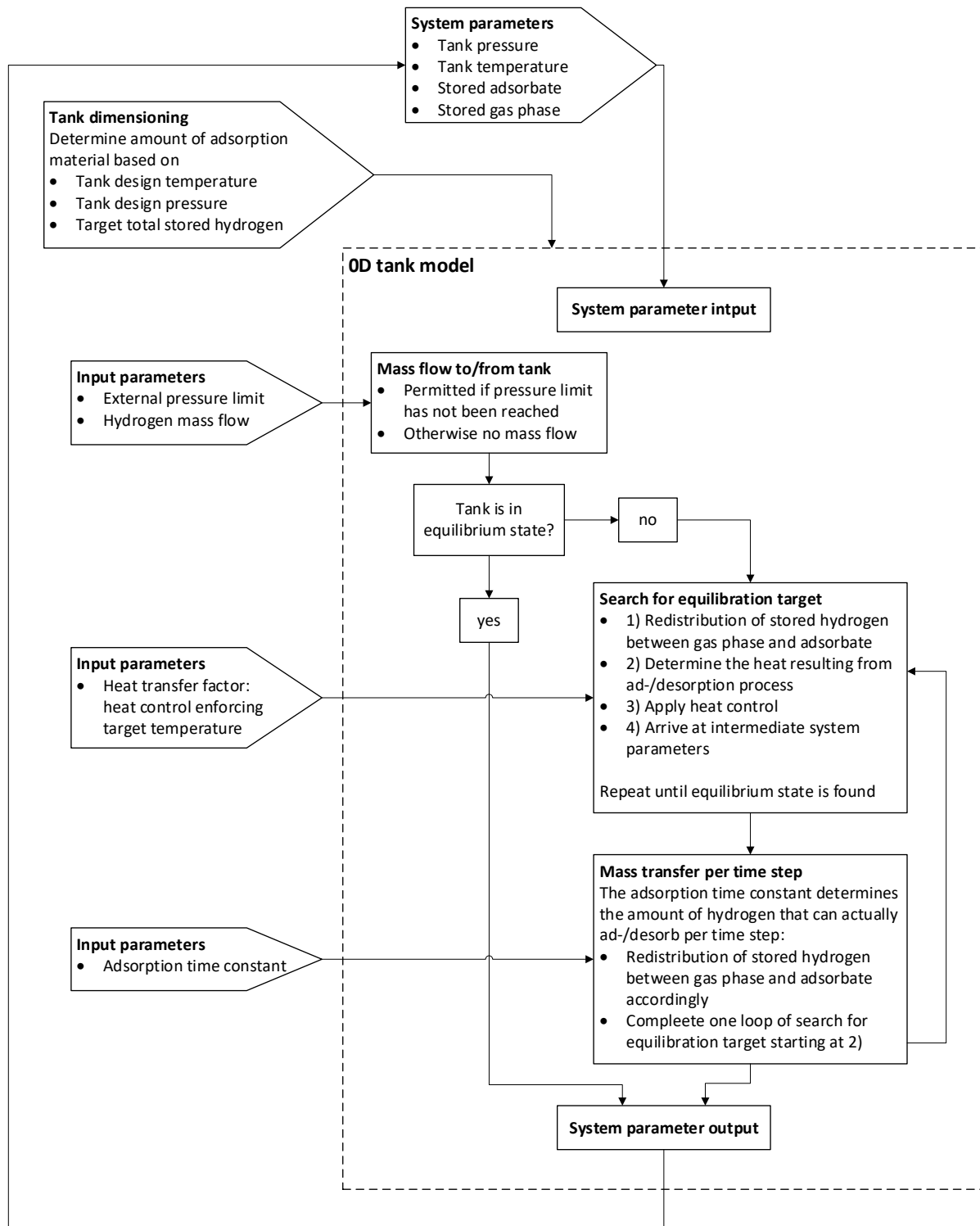


Figure 2: Block diagram of the adsorption storage simulation model.

### 2.2.1 Tank dimensioning and determination of system and input parameters

Before starting a simulation run, the tank dimension in respect to adsorbent mass is derived from the tank design parameters. For this reason, the tank design temperature, the tank design pressure and the target total stored hydrogen need to be defined. The tank, that is investigated

in this work, has the tank design parameters listed in Table 3. From these three parameters the amount of adsorption storage material inside the tank (referred to as the tank dimension) is calculated to be 20.36 kg.

From the system parameters tank temperature and tank pressure (Table 4) the stored mass of hydrogen can be calculated. The system parameters tank pressure and tank temperature at time step 0 (referred to as initial values), have to be set manually. At a time step larger than zero the system parameters (tank operation parameters) are calculated from the 0D tank model.

Table 3: Tank design parameters for tank dimensioning

| Tank dimensioning            |         |
|------------------------------|---------|
| Tank design temperature      | 77 K    |
| Tank design pressure         | 300 bar |
| Target total stored hydrogen | 5 kg    |

Table 4: System parameters for 0D tank model

| System parameters for 0D tank model |     |
|-------------------------------------|-----|
| Tank pressure                       | bar |
| Tank temperature                    | K   |
| Stored adsorbate                    | kg  |
| Stored hydrogen in gas phase        | kg  |

The stored mass is the sum of the stored adsorbate and the stored gas phase. The stored adsorbate is calculated from the D-A model fit of the adsorption isotherms of hydrogen on AX-21™ by inserting the fit parameters from Table 2 and the system parameters  $T$  and  $P$  into Equation (1). The stored gas phase ( $n_{gas}$ ) is calculated from the ideal gas equation by inserting the gas phase volume, the system parameters  $T$  and  $P$  and the universal gas constant. Both the equation for calculating  $n_{ads}$  and  $n_{gas}$ , are normalized to 1 kg of adsorption storage material. Therefore, they represent a specific hydrogen amount in respect to the storage material mass, and, have to be multiplied by the amount of adsorption storage material to determine the total stored hydrogen in the tank.

$$n_{gas} = \frac{P * 0.00147}{R * T} \quad (2)$$

The set of input parameters for the 0D tank model is listed in Table 5. From top to bottom, the external pressure limit denotes the maximum possible pressure with which the hydrogen mass flow can enter the tank. The heat transfer factor, a parameter that influences the temperature control, will be explained in more detail in Section 3.2. The target temperature is the set point for the system, to which the tank is cooled/heated by the temperature control. With an ideal temperature control the tank temperature (operation temperature) would always be equal to the target temperature. However, in a real system, with finite heating/cooling power and thermal resistance, the tank temperature will most of the time differ from the target temperature due to the released adsorption heat. The adsorption time constant regulates how much mass

can be actually adsorbed per time step. This will be covered in more detail in the Sections 2.2.4 and 3.4.

Table 5: Input parameters for 0D tank model

| Input parameters for 0D tank model |      |
|------------------------------------|------|
| External pressure limit            | bar  |
| Hydrogen mass flow                 | kg/h |
| Heat transfer factor               | W/K  |
| Target temperature                 | K    |
| Adsorption time constant           | 1/s  |

### 2.2.2 Condition for permitting mass flow into the tank and the check for equilibrium conditions

At the begin of every simulation run the tank pressure is checked against the external pressure. Only if the pressure limit has not been reached, mass flow into the gas phase of the tank is permitted. After this mass addition, the new gas phase pressure is calculated and the system parameters are checked against equilibrium conditions. If the tank is in equilibrium the calculation for one time step is finished, if not, the search for the equilibration target is triggered.

### 2.2.3 Search for equilibration target

The search for the equilibration target is an iterative process. Firstly, hydrogen is redistributed from/to the gas phase to/from the stored adsorbate. For an adsorption process small mass increments of hydrogen are transferred from the gas phase into the adsorbate. After every mass transfer the gas phase pressure and the equilibrium pressure (according to the D-A model at the current amount of stored hydrogen) are calculated. If these two coincide, the intermediate equilibrium is found. If not, the process is repeated. Secondly, the heat resulting from this step of ad- or desorption process (adsorption heat) towards the intermediate equilibrium is determined: the heat of ad-/desorption ( $\Delta H$ ) is calculated from Equation (3) (as found in Wang et al. [15]) and multiplied with the change in adsorbed hydrogen. Since the heat of adsorption also depends on the amount of stored adsorbate ( $n_{ads}$ ), the value of  $\Delta H$  changes over the state of charge of the tank.

$$\Delta H = \alpha \sqrt{\left[ \ln \left( \frac{n_{max}}{n_{ads}} \right) \right]} \quad (3)$$

$$\Delta T = \frac{\Delta H - Q}{c_{storage\ material} + c_{ads} + c_{gas}} \quad (4)$$

Thirdly, the temperature control ( $Q$ ) (heating/cooling) is applied, reducing the resulting total heat release by a certain amount. Combining the remaining heat, with the specific heat

capacities of the adsorption storage material ( $c_{storage\ material}$ ) [16], the adsorbed hydrogen ( $c_{ads}$ ) [17] and the hydrogen in gaseous form ( $c_{gas}$ ) [18] the temperature change in the tank ( $\Delta T$ ) is calculated (Equation (4) [19]). Consequently, all of these steps result in a change of the tank temperature and a set of intermediate system parameters. If the temperature change to that intermediate equilibrium is greater than zero, the tank pressure is adjusted as in section 2.2.2 and the iterative loop is repeated until the temperature change of a following loop is zero, the system has thus equilibrated and the search for the equilibration target is finished.

#### 2.2.4 Mass transfer per time step

In the final segment of the 0D model the mass transfer per time step is determined. In other words, how much hydrogen can actually be ad-/desorbed per timestep. The kinetic model used for this is the linear driving force model (Equation (5) [2]). It reduces the amount of adsorbate needed to directly reach the equilibrium, represented by the difference between the stored adsorbate before going into the search for the equilibration target ( $n_{ads\_start}$ ) and the stored adsorbate ( $n_{ads\_eq}$ ) at the target equilibrium, via the adsorption time constant  $k_L$  to calculate the actual possible change in stored adsorbate ( $\Delta n_{ads}$ ). The adsorption time constant can take values between 0 (no sorption happens in this time step) and 1 (the equilibration target is reached in this time step). [2] Thus, the amount of actual adsorbed hydrogen is always a fixed portion of the amount needed for reaching the equilibrium target in one step.

$$\Delta n_{ads} = k_L (n_{ads\_eq} - n_{ads\_start}) \quad (5)$$

The new amount of stored adsorbate is found by adding  $\Delta n_{ads}$  to  $n_{ads\_start}$ . Since the total stored mass is not changed the share of mass in the gas phase is redistributed accordingly. For this new mass distribution one loop of search for equilibration (Section 2.2.3) is performed (to take account for the changed parameters), starting at the determination of the adsorption heat. Finally, the new system parameters are found and the calculation for one time step is complete.

### 3 Results and discussion

Section 3 contains the results of the parameter studies on tank operation temperature and its effects on storage capacity, the influence of the temperature control on the adsorption behaviour, the changes of tank filling time with different mass flows and the influence of the adsorption time constant on the behaviour of stored adsorbate and stored gas phase. From these results basic necessary measures for the optimisations of real-world adsorption storage tanks can be derived. The tank under investigation has the design parameters specified in Table 3. The adsorption processes in section 3.1 to 3.3 are conducted with an adsorption time constant of 1. In Section 3.4 Adsorption processes for two different adsorption time constants are compared.

### 3.1 Effects of the target temperature on the total stored mass

As illustrated in Figure 1, the stored adsorbate does not only change with tank pressure but also with tank temperature. In Figure 3 it will be discussed what effects this behaviour has on adsorption storage tanks with different target operation temperatures.

From top row to bottom row, the subfigures of Figure 3 depict the system parameters such as the stored hydrogen mass (gas phase, adsorbate, total) (I), the tank pressure (II) and the tank temperature (III), as well as the heat control (IV). The red dotted line in (I) indicates the target total stored hydrogen mass of 5 kg. The total stored mass is always the sum of the stored gas phase and the stored adsorbate, as it is broken down in detail in (I).

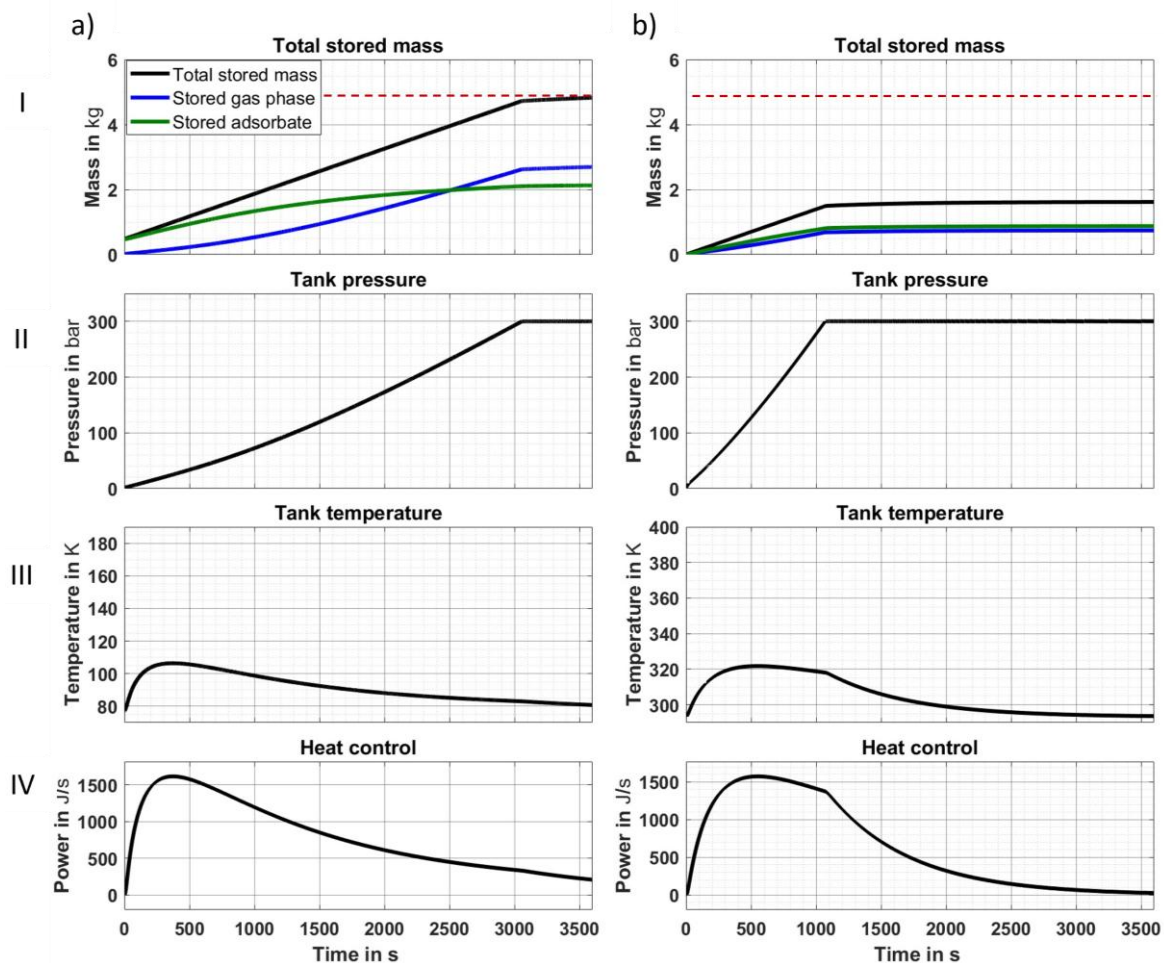


Figure 3: Two simulated adsorption processes for two different target temperatures of 77 K (a, left column), and 293.15 K (b, right column) and the corresponding system parameters total mass (I), tank pressure (II), tank temperature (III), heat control (IV)). Both processes are performed from 1 bar initial pressure to 300 bar external pressure limit, with a mass flow of 5 kg/h for 1h and the heat transfer (factor for heat control) set to 55 W/K.

Figure 3 (a, left column of subfigures) shows an adsorption process for a target temperature of 77 K, and Figure 3 (b, right column) for a target temperature of 293.15 K.

In row (I) of both columns the increase of total storage mass over time shows two distinct phases: in the “regular filling phase”, the total stored hydrogen increases linearly up to the

external pressure limit. In the “convergence phase”, after reaching the external pressure limit, the total stored hydrogen slowly converges to its final value.

Shown in Figure 3 (a, left column), the tank is operated at low operation temperature starting at 77 K (liquid nitrogen temperature), and is filled up to its tank design pressure of 300 bar. With these settings, starting from the initial total storage mass of 0.48 kg (at 1 bar), a total storage mass of 4.83 kg (at 300 bar) of hydrogen is reached after one hour. In the regular filling phase, the slope of the linear increase of total stored mass over time (I) is equal to the mass flow into the tank – the constant mass flow results in a constant slope.

In the beginning of the filling process the hydrogen is mostly adsorbed and thus stored as adsorbate. With increasing total stored mass, the share of the hydrogen stored in the gas phase increases and even surpasses the amount actually adsorbed on the material. Subfigure (a,II) depicts the respective tank pressure which shows a slightly convex behaviour up to the external pressure limit. This phenomenon will be revisited in Section 3.2. Subfigure (a,III) illustrates the temperature development of the tank. It shows a peak in temperature in the early stages of the adsorption process and a decrease back to the target temperature later on. This is a direct consequence of the saturation effect of the adsorption behaviour of hydrogen on activated carbon (see Figure 1). In the beginning of the adsorption process (at low total stored mass) the amount of hydrogen adsorbing per time is higher than for a tank that is almost filled to capacity, as can be seen in (a,I). Consequently, in the beginning of the filling phase more adsorption heat per time is released – the tank temperature rises significantly. Triggered by this temperature rise the heat control starts dissipating the adsorption heat to bring the tank back to its target temperature (IV). At the selected heat transfer factor of 55 W/K only a fraction of the adsorption heat can be cooled away and heat accumulation in the tank is observed. This results in the temperature rise depicted in (III). In the later stages of the regular filling phase the hydrogen adsorbed per time is lower than in the beginning. This leads to a smaller amount of adsorption heat released per time step. The heat control is able to catch up and dissipates the heat accumulation. The temperature is decreasing towards the target value. As a result, towards the end of the regular filling phase, the tank temperature has almost returned to its target temperature of 77 K.

After the external pressure limit is reached, the criterion for further mass flow is not fulfilled anymore. The tank pressure remains constant at 300 bar and the storage tank enters the slow convergence phase, in which the adsorption process is solely temperature driven. Since the tank temperature has not yet reached its target temperature the heat control stays active, dissipating the remaining adsorption heat. A drop in tank temperature results in a decrease of tank pressure. As soon as the tank pressure falls below the external pressure limit another mass increment of hydrogen can be added into the tank. Thus, the pressure increases again and the criterion for further mass flow is not fulfilled anymore. As long as the heat control is active and therefore the tank temperature is still decreasing this sequence is repeated. The resulting mass flow into the tank is strongly decreased in comparison to the regular filling phase and comes to a standstill when the tank reaches its target temperature.

Figure 3 (b, right column), shows the tank operated up to its tank design pressure of 300 bar but at a higher target temperature of 293.15 K. This temperature is far above the tank design temperature of 77 K, which has been discussed above. The effect of such high operation temperatures on the total stored mass can directly be observed in (b,I). The total stored mass

after one hour of adsorption amounts to 1.62 kg which is only a third of the total stored mass that was reached in (a,I). The behaviour of the two phases of column (b) follows the same principle as in column (a). However, due to the higher target temperature, the material is much faster saturated and more hydrogen remains in the gas phase. The external pressure limit in (b) is reached about three times faster than in (a).

At the beginning of the convergence phase the mass flow into the tank and consequently the adsorption rate is abruptly reduced (b,I). From this point onward the heat control starts dissipating the heat accumulation with only very little additional heat input into in the tank – the cooling power can be reduced significantly (b,IV).

As expected, operating an adsorption storage tank at temperatures below room temperature (ideally at liquid nitrogen temperature) leads to higher total storage capacities. On the one hand, more hydrogen gets stored as adsorbate, on the other hand, at lower temperatures, more hydrogen can be stored in the gas phase before reaching the external pressure limit than at room temperature. Thus, in order to efficiently (regarding storage capacity) operate the adsorption storage tank, it must be cooled below room temperature during the adsorption process.

### **3.2 Influence of the heat transfer factor on heat control**

As Section 3.1 has shown, a lower target temperature leads to more efficient hydrogen storage. To enforce target temperatures below room temperature, a heat control system is required. Depending on the level of optimization, the ability of the heat control to dissipate heat from the tank, will differ. The effects of these differences are discussed in this section.

From left (a) to right (c) Figure 4 shows adsorption processes with increasing heat transfer factors and thus more efficient cooling systems. The heat transfer factor correlates the heat transfer with the temperature difference between the target temperature and the tank temperature [10]. In other words, the higher the heat transfer factor the more heat can be dissipated away from or transferred into the tank for cooling and heating respectively. This heat control is depicted in row (IV) of Figure 4.

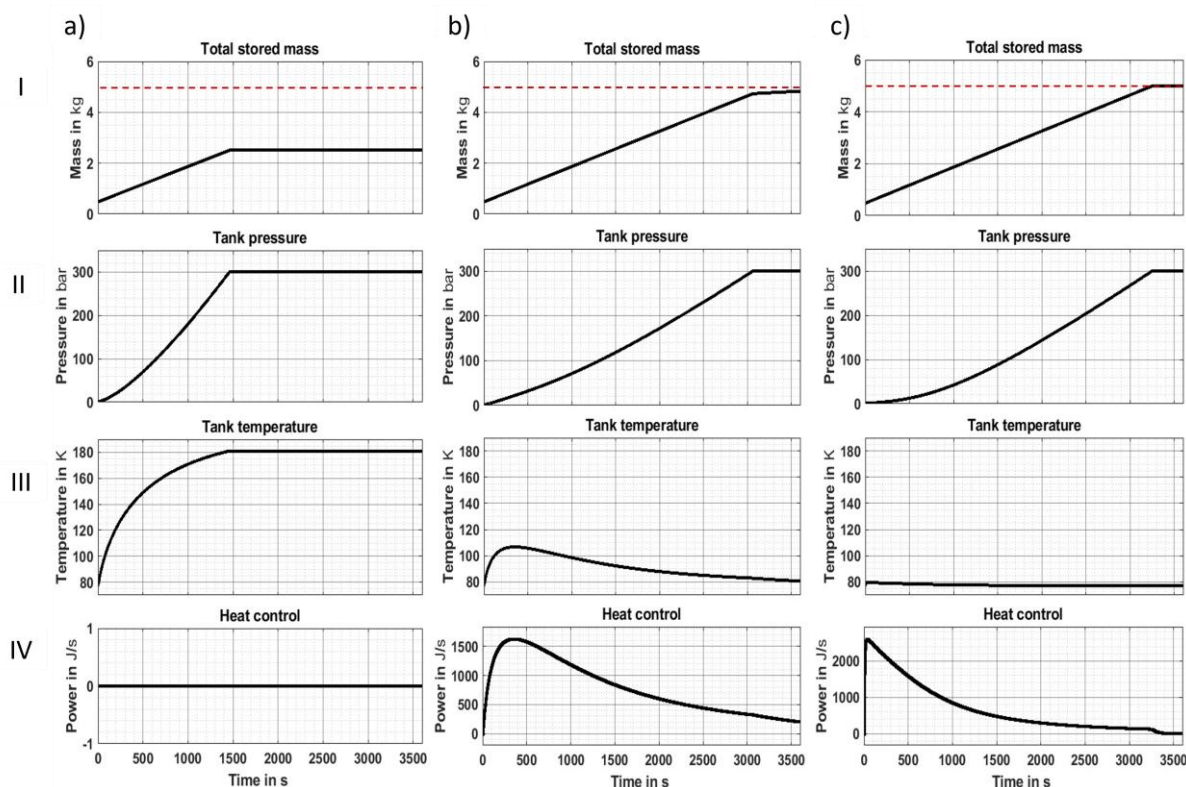


Figure 4: Three simulated adsorption processes for increasing heat transfer factors for heat control set to (a, left column) 0 W/K (adiabat), (b, middle column) 55 W/K, (c, right column) 1000 W/K. All adsorption processes are performed from 1 bar initial pressure to 300 bar external pressure limit with a mass flow of 5 kg/h for 1 h at a target temperature of 77 K.

In all three subfigure columns of Figure 4 hydrogen is adsorbed up to 300 bar at a target temperature of 77 K. However, only (c) can reach the target total stored mass of 5 kg after one hour (I). As can be seen in (b,I), the adsorption process with the second most efficient cooling system reaches 4.83 kg total stored mass, while the adsorption process shown in (a,I) reaches only 2.5 kg of hydrogen stored after one hour. This indicates that not only the target temperature and the external pressure limit play a role when it comes to total stored mass but also the heat control.

In column (a) the heat transfer factor is set to 0 W/K (IV). The adsorption process is adiabatic. This means that no heat is dissipated away from the tank and the tank temperature increases over time (III). With increasing tank temperature, the maximum adsorption capacity as well as the stored gas phase per pressure increment are going down, leading to a reduced total stored mass. Also, the external pressure limit is reached at an earlier point of the adsorption process than for lower tank temperatures.

In column (b) the heat transfer factor is set to 55 W/K (IV). Here a fraction of the adsorption heat can be dissipated every time step. After one hour of adsorption the tank temperature almost returns to the target temperature of 77 K (III). The tank pressure (II) increases slower than in (a,II). Consequently, before reaching the external pressure limit more hydrogen has been added into the tank (I) resulting in a higher total stored mass than in (a,I).

With the heat transfer factor set to 1000 W/K in column (c) the adsorption process is almost isothermal (c,III). The tank is operated close to its tank design temperature of 77 K and up to its tank design pressure of 300 bar (c,II). Hence, the target total stored amount of 5 kg can be reached within the time of one hour with a mass flow of 5 kg/h (c,I).

Revisiting the phenomenon of convex behaviour of the pressure change over time, briefly mentioned in section 3.1: Regarding the fact, that the tank is filled at constant mass flow one would expect a linear increase in tank pressure. However, the situation for an adsorption storage tank is different in respect to the two counteracting processes at play: on the one hand, the change of tank pressure due to changes in tank temperature (also at constant stored gas phase), on the other hand the steeper increase of stored adsorbate in early stages of the adsorption isotherm compared to later on, when the tank is almost filled to capacity (see Figure 1 or Figure 3 (a,I)).

Starting with the latter, Figure 4 (c,II) shows the tank operated almost isothermally, which means that the deviation from a linear relation between pressure and time can only result from the distribution of the total stored mass between stored adsorbate and stored gas phase. In the early stages of the adsorption process a major part of the total stored mass is present as stored adsorbate. Only a small fraction is stored in the gas phase. Hence, the tank pressure is small. This explains why the total stored mass (as the sum of adsorbate and gas phase) can increase linearly although the pressure increases less than proportionately. At later stages of the adsorption process the adsorption rate slows down and a larger share of the total stored mass is stored in the gas phase.

In contrast to column (c) where the temperature is almost constant (close to ideal cooling), column (b) experiences temperature changes over the evaluation period (c,III) like in a realistic cooling scenario. The convex behaviour of the pressure curve, due to differing adsorption rates over time (as in (c,II)), is now mitigated by the tank temperature increase (b,II). A higher tank temperature results not only in a rising tank pressure, but also in a reduction in stored adsorbate. Consequently, a small fraction of stored adsorbate gets redistributed to stored gas phase increasing the tank pressure even further. This becomes apparent when comparing (b,II) and (c,II) where both curves show convex behaviour. However, taking a closer look at the first 500 s, the pressure in (b,II) (not in isothermal condition) is distinctly higher than in (c,II) (close to isothermal condition).

To conclude, for maximizing the storage capacity of an adsorption tank, the heat control system has to be optimized towards high thermal conductivity. Otherwise, the target operation temperature cannot be enforced. The tank temperature rises and the total storage capacity is reduced.

### **3.3 Effects of different mass flows on the filling time**

Sections 3.1 and 3.2 both discussed adsorption tanks at a mass flow of 5 kg/h. In contrast, in this section the effects of different mass flows on otherwise identical adsorption tanks are investigated. From top to bottom, the rows of subfigures (a) to (d) of Figure 5 show adsorption processes with a higher mass flow each. The sequence of subfigures follows the same concept as in the previous sections with the rows and columns flipped. This is done for easier comparison of the different behaviours of the system parameters over time. The red dotted line

in column (I) still denotes the target total stored mass of 5 kg, the blue dotted line indicates the half filling of 2.5 kg.

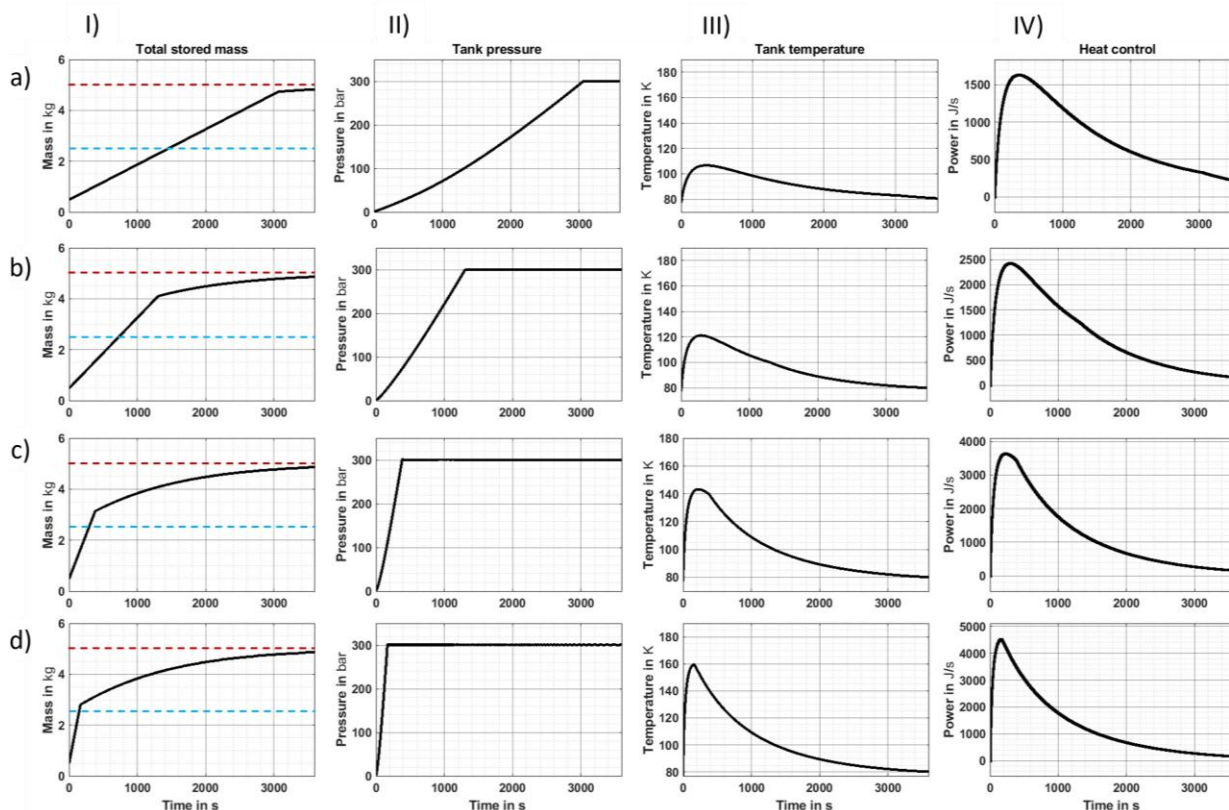


Figure 5: Four simulated adsorption processes with different mass flow of 5 kg/h (a, first row), 10 kg/h (b, second row), 25 kg/h (c, third row), 50 kg/h (bottom row). All adsorption processes are performed from 1 bar initial pressure to 300 bar external pressure limit for 1 h at a target temperature of 77 K and the heat transfer factor for heat control set to 55 W/K.

The first row (a) depicts an adsorption process with a mass flow of 5 kg/h. The features of this adsorption process have already been discussed in the previous sections in Figure 3 (a) and Figure 4 (b). Row (a) will be our reference to compare the other rows of subfigures (b) to (d). We will discuss Figure 5 from left (column I) to right (column IV) comparing and contrasting the different effects the change in mass flow has on the system parameters.

Starting with column (I), the mass flow has only very little influence on the final total stored mass after one hour. It ranges from 4.82 kg in (a,I) to 4.87 kg in (d,I). However, the evolution of total stored mass within this one hour varies considerably between the four rows of subfigures. As can be seen at the points of intersection between the blue dotted line (tank is half full) and the evolution of the total stored mass, higher mass flow causes the tank to be much faster half-filled. This is a direct consequence of the total stored mass, rising with a slope equal to the incoming mass flow – higher mass flow results in steeper increase of total stored mass. In (a,I) 2.5 kg total stored mass (half filling) is reached after 24 minutes, and for (b,I), (c,I) and (d,I) after 12 minutes, 5 minutes and 2 minutes respectively. With increasing mass flow, the external pressure limit is also reached faster (column II), and the regular filling phase transitions earlier into the convergence phase. Two factors are responsible for this: firstly, the stored gas phase per time rises from (a) to (d). Secondly, higher mass flow leads to higher adsorption rates, leading to a more rapid temperature increase (column III), as already

discussed in the previous sections. Attempting to dissipate the heat accumulation inside the tank, the heat control power increases from (a,IV) to (d,IV).

The key message of Figure 5 is that the time, after which the target total stored mass is reached, is not directly proportional to the mass flow. At finite heat dissipation, the increase of total stored mass is limited by the tank temperature – the system is self-inhibiting. Consequently, increasing the mass flow does not lead to a faster filling time when loading the tank fully, it merely requires the heat control to be operate with higher power to counteract the adsorption heat and the tank is faster transitioning to a slow convergence phase. On the other hand, the mass flow has a significant influence when considering a partial, e.g. a 2.5 kg hydrogen filling.

### **3.4 Influence of the adsorption time constant on the ratio between stored adsorbate and stored gas phase**

The adsorption processes discussed in the previous sections all had the adsorption time constant set to 1. This means that in every time step the equilibration target has been reached. With an adsorption time constant smaller than 1 (in the following case a value of 0.1 was chosen), the amount of hydrogen actually adsorbing per time step is reduced to 10% compared to the amount of hydrogen that would adsorb, such that the equilibration target for this time step would be reached. This is illustrated in Figure 6 where the amount of stored adsorbate (left) and the amount of stored gas phase (right) is shown in comparison between two processes with adsorption time constants of 1 (magenta) and 0.1 (blue).

While the curve of stored adsorbate (blue), not reaching equilibrium conditions every time step, lies below the curve for the stored adsorbate which is always in equilibrium (magenta), the gas phase curve shows the opposite behaviour.

To understand this pattern, it has to be understood that the hydrogen mass flow entering the tank is initially added to the gas phase and only then a certain amount of hydrogen (depending on the adsorption time constant) is adsorbed onto the storage material. The rest of the hydrogen remains in the gas phase. During the regular filling phase both increase steadily.

In the subsequent convergence phase (after the external pressure limit is reached) the stored gas phase shows a kind of sawtooth pattern. The peak of a sawtooth indicates that the external pressure limit has been reached and no more mass flow is permitted into the tank until the gas phase pressure falls below the limit again due to a slow adsorption process of gaseous hydrogen, onto the storage material. This process is indicated by the falling edges of the sawtooth pattern (Figure 6, right, blue) which follows an exponential decay. It can take several time steps until the tank pressure is again below the external pressure limit and one portion of mass flow is again permitted into the tank.

This process continues until the tank pressure can no longer fall below the external pressure limit and no mass flow is added anymore. With the total stored mass now remaining constant, the curves for stored hydrogen and stored hydrogen in and out of equilibrium begin to converge and will reach the same value after a certain period (not shown in Figure 6).

To summarize, the choice of the adsorption time constant greatly influences the ratio of stored adsorbate to stored gas phase.

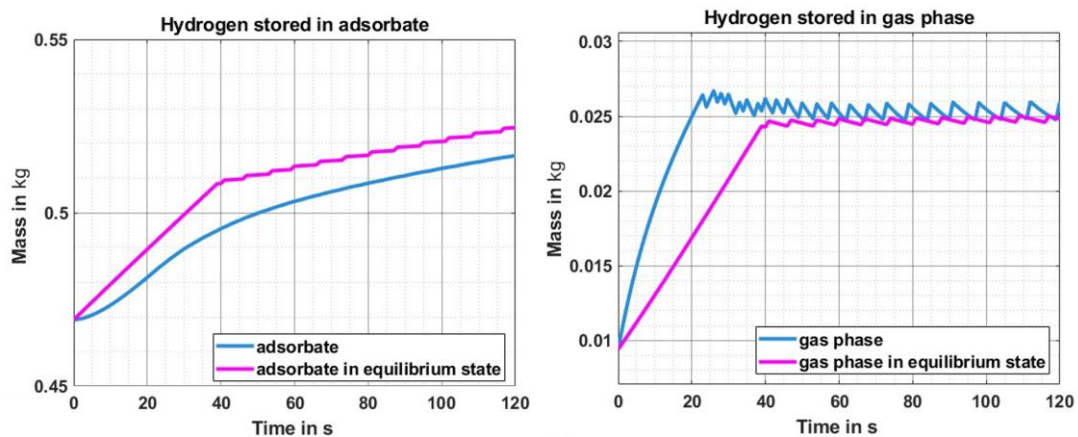


Figure 6: Two simulated adsorption processes showing the stored adsorbate (left) and the stored gas phase (right) for different values of the adsorption time constant: target equilibrium state ( $k_L = 1$ ) in magenta and actual amount of hydrogen ( $k_L = 0.1$ ) in blue

Both adsorption processes are conducted between 1 bar to 3 bar external pressure limit for 120 s (equals 2 minutes) at a target temperature of 77 K and the heat transfer factor for heat control set to 55 W/K and a mass flow of 5 kg/h.

## 4 Conclusion

The MATLAB Simulink 0D tank model allows for a quick estimate of the interrelations of the parameters tank temperature, temperature control, storage capacity, mass flow and filling time. The results of the parameter studies show that, in order to efficiently (regarding storage capacity) operate an adsorption storage tank, the tank must be cooled below room temperature during the adsorption process. To achieve these low operation temperatures, the temperature control system has to be optimized towards high thermal conductivity. In a real-world tank the heat dissipation through the temperature control is, even if optimized, still finite. Since the increase of total stored mass is limited by the tank temperature, increasing the mass flow does not lead to a faster filling time when loading the tank fully. However, it has a significant influence when considering a partial tank filling and dynamic operation. For an adsorption process in which the equilibration target cannot be reached for every time step, the choice of the adsorption time constant affects the ratio of stored adsorbate to stored gas phase and influences the adsorption kinetics significantly.

## 5 Outlook

In the next step the simulation model will be validated, on the one hand, with literature data and, on the other hand, with data obtained from adsorption experiments. These will be performed in-house at our adsorption storage test bench, which is currently under construction.

## 6 References

- [1] M.-A. Richard et al., "Gas adsorption process in activated carbon over a wide temperature range above the critical point. Part 1: modified Dubinin-Astakhov model", *Adsorption*, pp. 43-51, 2009. DOI 10.1007/s10450-009-9149-x.
- [2] L. Chen et al., "Modeling adsorption-based hydrogen storage in nanoporous activated carbon beds at moderate temperature and pressure", *International Journal of Hydrogen Energy*, pp. 159–179, 2025, DOI 10.1016/j.ijhydene.2025.03.373.

- [3] N. Klopčič, "Advancing hydrogen storage technologies and infrastructures", 2024, Institute of Thermodynamics and Sustainable Propulsion Systems, DOI 10.3217/R6BFQ-FR092.
- [4] US Department of energy, Hydrogen Storage, available online <https://www.energy.gov/eere/fuelcells/hydrogen-storage#:~:text=On%20a%20mass%20basis%2C%20hydrogen,meet%20DOE%20hydrogen%20storage%20targets>. last checked 28.01.2026
- [5] S. Stock et al., "Coffee Waste-Derived Nanoporous Carbons for Hydrogen Storage", ACS Applied Energy Materials, pp. 10915–10926, 2022, DOI 10.1021/acsaem.2c01573.
- [6] Y. Wen et al., "Advances in hydrogen storage materials for physical H<sub>2</sub> adsorption", International Journal of Hydrogen Energy, pp. 1261–1274, 2025, DOI 10.1016/j.ijhydene.2024.11.459.
- [7] L. A. M. Mahmoud et al., "Porous carbons: a class of nanomaterials for efficient adsorption-based hydrogen storage", RSC Applied Interfaces, pp. 25–55, 2025, DOI 10.1039/d4lf00215f.
- [8] G. Sdanghi et al., "Modelling of a hydrogen thermally driven compressor based on cyclic adsorption-desorption on activated carbon", International Journal of Hydrogen Energy, pp. 16811–16823, 2019, DOI 10.1016/j.ijhydene.2019.04.233.
- [9] N. Kostoglou et al., "Effect of Pt nanoparticle decoration on the H<sub>2</sub> storage performance of plasma-derived nanoporous graphene", Carbon, pp. 294–305, 2021, DOI 10.1016/j.carbon.2020.08.061.
- [10] N. Klopčič et al., "Simulation toolchain for the development of metal hydride storage systems", International Journal of Hydrogen Energy, pp. 393–408, 2025, doi.org/10.1016/j.ijhydene.2025.03.186.
- [11] N. Kostoglou et al., "Nanoporous polymer-derived activated carbon for hydrogen adsorption and electrochemical energy storage", Chemical Engineering Journal, pp. 131730, 2022, DOI 10.1016/j.cej.2021.131730.
- [12] B. Panella, "Hydrogen Storage by Physisorption on Porous Materials", 2006, Max-Planck-Institut für Metallforschung.
- [13] L. Torrisi et al., "Measurements on Five Characterizing Properties of Graphene Oxide and Reduced Graphene Oxide Foils", Physica Status Solidi A, 2022, DOI 10.1002/pssa.202100628.
- [14] R. Checchetto et al., "Sievert-type apparatus for the study of hydrogen storage in solids", Measurement Science and Technology, pp. 127–130, 2004, DOI 10.1088/0957-0233/15/1/017.
- [15] J. Wang et al., "Integrated targeted pre-cooling tubes and fins for enhanced hydrogen adsorption in activated carbon storage tank", International Journal of Hydrogen Energy, 2025, DOI 10.1016/j.ijhydene.2025.06.132.
- [16] S. Mann et al., "Thermodynamic properties of pure and doped (B, N) graphene", RSC Advances, pp. 12158–12168, 2016, DOI 10.1039/c5ra25239c.
- [17] V. G. Jervell, "Thermodynamic Properties of Hydrogen Adsorbed on Graphite Surfaces at Temperatures Above 100 K: A Molecular Dynamics and Classical Density Functional Theory Study", Entropy, 2025, DOI 10.3390/e27020184.
- [18] U.S. Secretary of Commerce on behalf of the United States of America, NIST Chemistry WebBook, Hydrogen, (NIST-JANAF Thermochemical Tables, Fourth Edition), available online <https://webbook.nist.gov/cgi/cbook.cgi?ID=C1333740&Type=JANAFG&Table=on#JANAFG>, last updated 2025, last checked 25.01.2026
- [19] M. Klell et al., "Wasserstoff in der Fahrzeugtechnik", Springer Fachmedien Wiesbaden, 2018, ISBN 978-3-658-20446-4, DOI 10.1007/978-3-658-20447-1.